Performance Analysis of Scramjet Engines

Performance Analysis of Scramjet Engines

Yoshiharu TSUJIKAWA*, Yujiro TSUKAMOTO** and Shoichi FUJII***

(Received June 16, 1988)

In order to propel a vehicle at hypersonic speeds, a supersonic combustion ramjet engine which consists of the inlet, combustor and nozzle can be regarded as a most promising one. The optimum configuration must be determined for given flight conditions.

In the present study, the quasi-one dimensional flow model through the scramjet engine is proposed and the performances of the components are analyzed thermodynamically. In the analysis, there is most severe difficulties in the combustor due to the problem such as turbulent diffusion and mixing at supersonic speed range. For the combustion reaction, the global hydrogen-air combustion model with two step reaction schemes of hydrogen and oxygen are introduced. To estimate the demerit of weight increase, the axial length of the components is calculated, which presented the basic information about the optimum configuration of the scramjet engine.

1. Introduction

The design of efficient hypersonic ramjet engines, where the primary mode of combustion occurs in a supersonic rather than a subsonic air streams, requires special consideration in a number of areas not normally considered in the design of conventional subsonic combustion ramjets. Specifically, if a supersonic combustion ramjet (SCRAMJET) engine is to fly over a reasonable Mach number range, e.g., $M_0 = 4 - 10$, the area-contraction ratio of the inlet-diffuser and the cross-sectional area ratio between combustor-inlet and exit and area distribution of the combustor must be selected to meet the low Mach number performance requirements yet permit good engine performance at the high Mach number cruise condition. The geometric optimization, therefore, is urgently required. So far, there have been a few attempts to optimize it. For example, Waltrup *et al.*[1] have optimized the design of scramjet engines including cycle analysis and Billig[2] has modified the geometric configuration of the experimental combustor model. Since both have used the Crocco power law relationship between static pressure and area, i.e. $PA^{\epsilon/(\epsilon-1)}$ = const. to analyze the combustor, no information have been obtained about axial length.

The numerical calculation of the turbulent mixing and reaction of fuel in the supersonic flow through a scramjet combustor is a computational problem of considerable interest. The introduction of detailed chemical reaction mechanisms into theoretical analyses of complex turbulent mixing flows often results in excessive computer run times and storage requirement. In the present study, therefore, some simplifications

* Department of Aeronautical Engineering, College of Engineering.
** Mitsubishi Heavy Industries Ltd., Komaki, Aichi.
*** National Aerospace Laboratory, Chofu, Tokyo.

have been employed. One such attempt is that chemical reaction occurs by means of an arbitrary postulated, onestep, irreversible reaction. It is also assumed that this reaction occurs very rapidly, the problem reduces to one in which the rate of combustion is entirely mixing controlled. A related concept involves the assumption that the fuel and oxidizer react instantaneously and form reaction products in chemical equilibrium.

The order of presentation will be to first design an optimum engine geometry using the established components norms and then to illustrate and discuss the sensitivity of this engine design to variations of inlet efficiency, combustor length and thermochemistry.

2. Analysis

The schematic presentation of the scramjet engine used in this study is shown in Fig. 1, and is a generic derivation of some recent scramjet powered vehicle concepts. For simplicity, and to be consistent with some of the engine configurations that have been proposed, it is assumed that the scramjet inlet is located beneath the main body and sufficiently far aft that the effects of forebody compression are negligible.

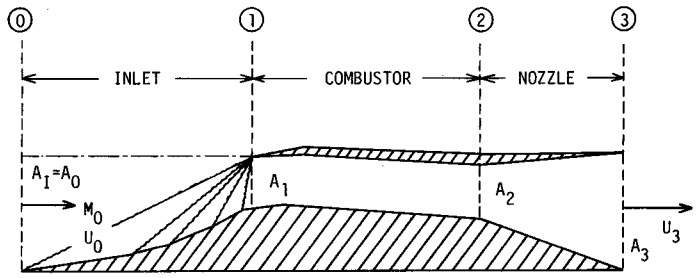

Fig. 1 Schematics of scramjet engine.

2.1. Inlet

Schematics of external compression inlet is shown in Fig. 2. The air capture ratio A_0/A_I is a function of flight Mach number, where A_I denotes the cross-sectional area of inlet. For simplicity, it is assumed to be unity in the present analysis. Multi-oblique

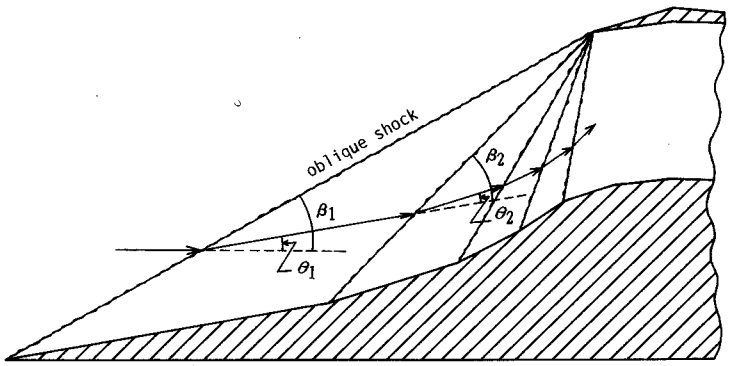

Fig. 2 Schematics of external compression inlet.

shock external compression inlet is adopted. The pressure recovery factor through one oblique-shock stage, therefore, is expressed by

$$\frac{p_{t_2}}{p_{t_1}} = \left(\frac{2\gamma}{\gamma+1} M_1^2 \sin^2\beta - \frac{\gamma-1}{\gamma+1} \right)^{-1/(\gamma-1)} \left[\frac{\{(\gamma-1)/2\} M_1^2 \sin^2\beta + 1}{\{(\gamma-1)/2\} M_1^2 \sin^2\beta} \right]^{-\gamma/(\gamma-1)} \tag{1}$$

The optimum shock angle, β_{iopt} and deflection angle, θ_{iopt} for each stage can be obtained by optimization procedure with multiplier method[3,4]. The axial length of inlet, therefore, is written as

$$x_I = d_0/\tan\beta_1 \tag{2}$$

2.2. Combustor

The combustion chamber must be designed to match the mixing process which is gradual and stable because the flow is supersonic. The main requirements of a supersonic combustion ramjet of this type is that the reaction rates which control the chemical reactions be very fast so that the mixing of fuel and oxidizer can be a much slower process and, therefore, be a rate-determining process. The turbulent mixing at supersonic speed range is affected by the method of fuel injection and accompanied with the complicated shock structure and intense interferences by air. The analytical study is very difficult, so that the data obtained from the experiment must be fed back into the analysis. The simplified model is made up with the following assumptions as:

(1) The fuel (hydrogen) is injected coaxially with the same temperature, pressure and velocity as air.
(2) The perfect mixing length is given in advance.
(3) For every calculation steps Δx, the quantities of air and hydrogen to react are newly given and they are perfectly stirred before the onset of reaction.
(4) After every steps, temperature, pressure and velocity are readjusted.
(5) The whole combustion reaction occurs at supersonic speed range.

The hydrogen-air combustion model is shown in Fig. 3. The following two-step global model for H_2 combustion is adopted[5],

$$H_2 + O_2 \xrightarrow{k_{f1}} 2OH \tag{3}$$

$$2OH + H_2 \xrightarrow{k_{f2}} 2H_2O \tag{4}$$

with the forward reaction rate constants given in the form of an Arrhenius equation

$$k_{fi} = A_i(\phi)\, T^{Ni} \exp(-E_i/RT) \tag{5}$$

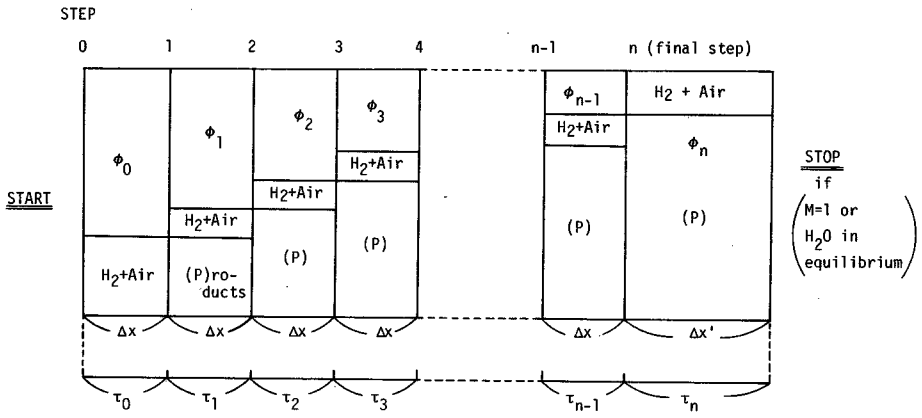

Fig. 3 Hydrogen-air combustion model.

where the pre-exponential $A_i(\phi)$ is a function of equivalence ratio. Values of parameters were established for reaction (3) and (4), and shown in Table 1 for initial temperature of 1000 – 2000K and equivalence ratios 0.2 – 2.0.

The typical results of this numerical calculation is that the mass fraction history of OH rises rapidly until a time, i.e. typically on the order of 10^{-10}s. At this point the rate of production of OH is near zero and the OH formation reaction is essentially in equilibrium. The amount of water produced at this point is a mass fraction of about 10^{-7}.

Table 1 Reaction rate constants and equilibrium constants.

K_{f1}	$A_1(\phi) = (8.917\phi + 31.433/\phi - 28.95) \times 10^{47}$ $E_1 = 4865$ $N_1 = -10$
K_{f2}	$A_2(\phi) = (2.0 + 1.333/\phi - 0.833\phi) \times 10^{64}$ $E_2 = 42500$ $N_2 = -13$
K_1	$26.164 \exp(-8992/T)$
K_2	$2.682 \times 10^{-6}\ T \exp(69415/T)$

The conservation equations are represented as follows:

Mass:

$$\mathrm{d}(\rho UA) = 0 \tag{6}$$

Momentum:

$$\mathrm{d}(\rho UAU) = 2\pi r (p \sin\alpha_C - \tau_W \cos\alpha_C)\,\mathrm{d}x - \mathrm{d}(pA) \tag{7}$$

Energy:

$$\mathrm{d}(\rho UAh) = -\rho U^2 A\mathrm{d}U + \dot{m}_r h_{H_2O} w\mathrm{d}x/U \tag{8}$$

where α_c, $\dot{m}_r$ and h_{H_2O} represents the angle of divergence of the combustor, a mass flow of reactants and lower heating value of hydrogen per unit mass of water, respectively. Combining them, the following equations are given

$$(\dot{m}_0 - \frac{\sigma T}{U^2})\,dU + \frac{\sigma}{U}\,dT = 2\sqrt{\pi A}\,(p\sin\alpha_C - \tau_w\cos\alpha_C)\,dx$$

$$- p\,dA + \frac{\sigma T\,dA}{UA} \tag{9}$$

$$\dot{m}_0 U\,dU + \dot{m}_0 Cp\,dT = \dot{m}_r h_{H_2O} w \frac{dx}{U} \tag{10}$$

where

$$\sigma = \dot{m}_0 R_0 \Sigma\,(y_i/w_i) = \dot{m}_0 R_0/M = \dot{m}_0 R$$

$$\dot{A} \equiv \frac{dA}{dx} = A_0\beta_C$$

$$\tan\alpha_C = \frac{dr}{dx} = \frac{\dot{A}}{2\sqrt{\pi A}}$$

Expressing the equations (9) and (10) as

$$D_1\,dU + D_2\,dT = D_3 \tag{11}$$

$$D_4\,dU + D_5\,dT = D_6 \tag{12}$$

Finally the following autonomous system of two first-order equations are obtained.

$$\frac{dU}{dx} = \frac{D_2D_6 - D_3D_5}{D_2D_4 - D_1D_5} \tag{13}$$

$$\frac{dT}{dx} = \frac{D_3D_4 - D_1D_6}{D_2D_4 - D_1D_5} \tag{14}$$

Numerical solution was obtained using a Runge-Kutta-Gill method.

2.3. Engine performance

In the nozzle, calculations were made for frozen-nozzle expansions – i.e., the compositions in the expansion process is fixed at that corresponding to equilibrium at the combustor exit.

Engine thrust is expressed by

$$F = \lambda\,(\dot{m}_a + \dot{m}_f)\,U_3 - \dot{m}_a U_0 \tag{15}$$

where $\lambda = (1 + \cos\alpha_N)/2$. The specific impulse is shown as

$$I_{sp} = F/(\dot{m}_f g) \tag{16}$$

3. Results and Discussions

3.1. Inlet

In the present study, since only external compression is adopted, much better pressure recovery can be obtained by taking advantage of a characteristics of shock waves: for a given Mach number, a series of weak shocks produces much less stagnation pressure loss than one strong shock. The pressure recovery factor versus combustor-inlet Mach number with the number of oblique shocks as parameter is shown in Fig. 4 for $M_0 = 9$. The axial length of inlet is shown in Fig. 5. From these figures, the further gains are obtained by introducing more oblique shocks. The penalty in weight due to more complicated mechanics, however, is inevitable.

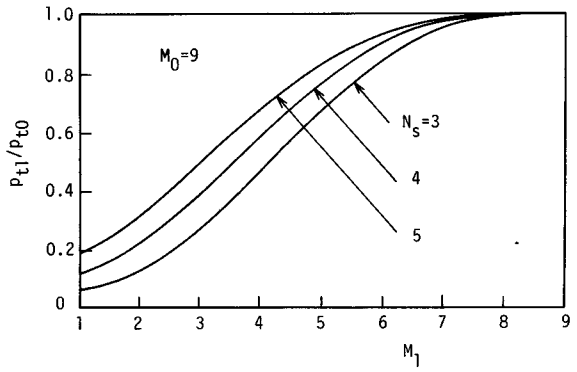

Fig. 4 Pressure recovery factor.

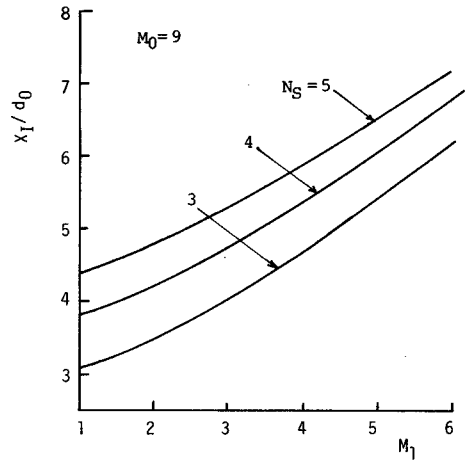

Fig. 5 Axial length of inlet.

3.2. Combustor

Since the combustion reaction is assumed to proceed entirely in supersonic speed range, the combustor-inlet Mach number must be high, e.g. $M_1 > 2$ so that the choking due to heat addition might not occur. In the present model, the loss of momentum due to turbulent mixing is neglected, so only the axial length of combustor, the area-distribution rate and area-ratio between combustor-inlet and exit can be regarded as variables. Among them the following relation can be formed.

$$A_2/A_1 = 1 + \beta_C x_C \tag{17}$$

As mentioned later, since the axial length of combustor is determined by the rate of turbulent mixing, the combustor-area-ratio is optimized for given combustor-inlet Mach number and equivalence ratio.

3.2.1. Mixing rate and perfect mixing length

The perfect mixing length x_{MIX}, which represents the distance required to realize a well stirred mixture, must be given in advance. It is closely related to the mixing rate. In the present study, it is non-dimensionalized by combustor-inlet diameter. It is depicted in Fig. 6 for $x_{MIX}/d_1 = 5$. Mixing length increases with combustor-inlet Mach number, since area-contraction of inlet also increases. In this model hydrogen is assumed to be injected coaxially with same temperature, pressure and velocity as air, so that the combustor-inlet diameter increases with the equivalence ratio. This model, therefore, has characteristics that for the same mixing rate the perfect mixing length increases in keeping with combustor-inlet Mach number and equivalence ratio. Actually, the assumption that when the mixing rate is constant, the mixing length becomes longer for high flow velocity is regarded to be reasonable.

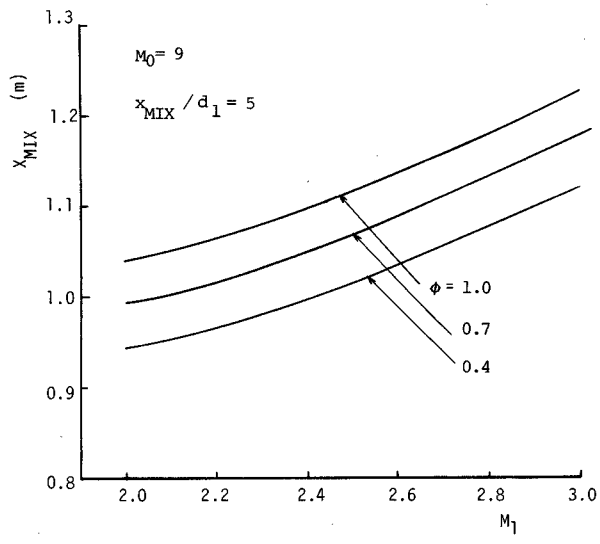

Fig. 6 Perfect mixing length.

3.2.2. Effects of mixing rate

It is aforementioned that the mixing is rate-determination process. To verify it, the combustor length for premixed case ($x_{MIX}= 0$), is shown in Fig. 7. The minimum combustor length is obtained for slightly larger value than stoichiometric equivalence ratio. The increase of area-distribution rate reduces the combustor length. In either case, it is considerably short. It is necessary to include the effects of the mixing process in the analysis. Those on combustor length are shown in Fig. 8. Time required for combustion strongly depends on the mixing process. Unfortunately, the analysis of turbulent mixing presents a difficult problem because of the lack of a basic formulation of the transport properties of hydrogen-air mixture. The engine performance is deteriorated obviously due to increase of wall shear.

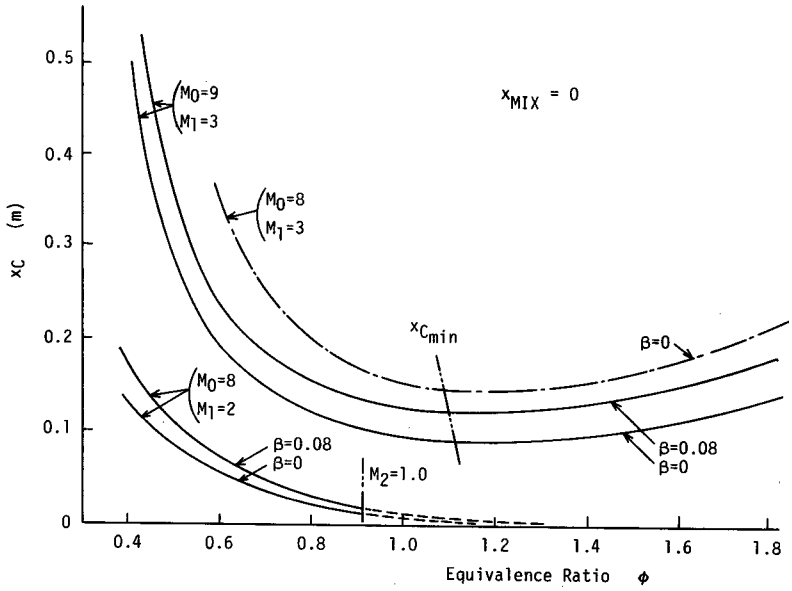

Fig. 7 Axial combustor length for premixed mixture.

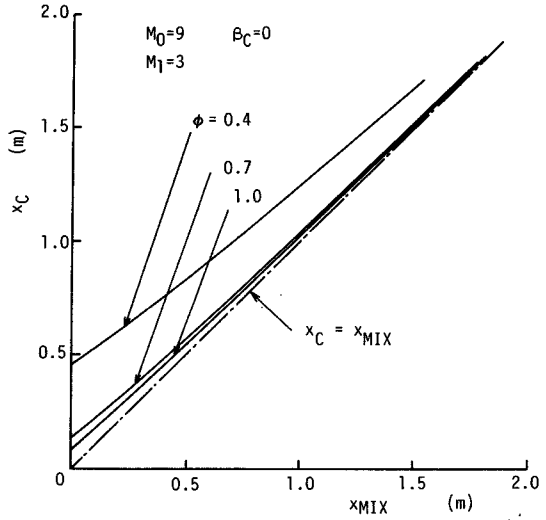

Fig. 8 Variation of combustor length with mixing length.

3.2.3. Area-distribution rate

As mentioned above, the perfect mixing length does not affect the engine performance. If combustor-area-ratio is constant, the combustor is more effective for less area-distribution rate. To clarify the effects of area-distribution rate, the following model is considered. With given combustor-area-ratio, the combustor axial length can be determined for area-distribution rate. Then, mixing length is assumed to be 80% of combustor length and wall shear is neglected. The combustion reaction is rapidly completed and every species are approximately in equilibrium at combustor-exit. The specific impulse vs. area-distribution rate is indicated in Table 2. The engine performance is improved with the decrease of area-distribution rate. The weight penalty, however, should be taken into consideration.

Table 2 Effects of area-distribution rate on engine performance.

ϕ	A_2/A_1	β_C	x_C (m)	I_{sp} (s)
0.7 $M_1 = 2.4$	1.5	0.5	1.0	2728.08
		1.0	0.5	2717.04
		1.5	0.333	2701.46
		2.0	0.25	2673.96
	2.0	0.5	2.0	2782.74
		1.0	1.0	2764.05
		1.5	0.667	2740.16
		2.0	0.5	2713.84
1.0 $M_1 = 3.0$	1.5	0.5	1.0	2296.22
		1.0	0.5	2273.77
		1.5	0.333	2242.27
		2.0	0.25	2153.55
	2.0	0.5	2.0	2328.30
		1.0	1.0	2296.53
		1.5	0.667	2258.98
		2.0	0.5	2222.43

$M_0 = 9$

3.2.4. Combustor-area-ratio

In the present calculation model, since the combustor axial length can not be given in advance, the combustor-area-ratio is still undetermined. A new parameter i.e. A_{MIX}/A_1, therefore, should be introduced. The effects of this parameter on the specific impulse is shown in Fig. 9 for $x_{MIX}/d_1 = 5$. As mentioned in section 3.2.1, the combustion reaction is very rapid, A_{MIX}/A_1 differs slightly from combustor-area-ratio. The relation of them is depicted in Fig. 10. From this figure, the optimum area-ratio can be obtained versus combustor-inlet Mach number, which is indicated in Fig. 11. As the

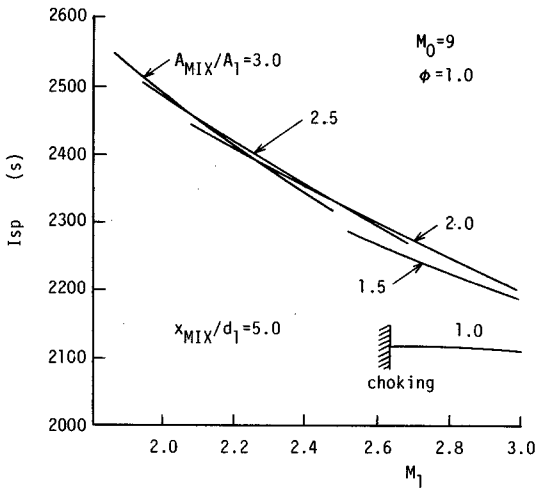

Fig. 9 Variation of specific impulse with combustor-inlet Mach number.

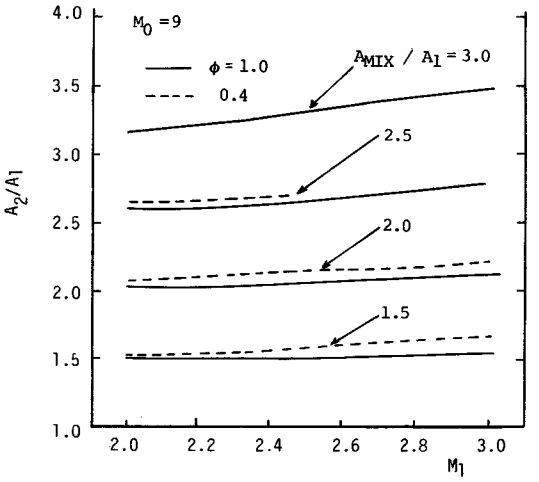

Fig. 10 Effects of A_{MIX}/A_1 on combustor-area-ratio.

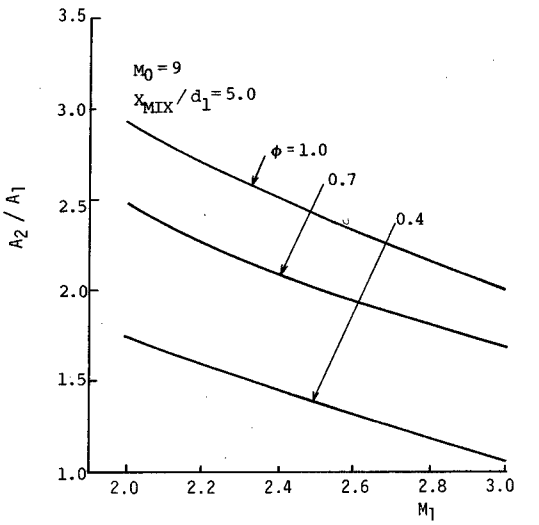

Fig. 11 Optimum combustor-area-ratio.

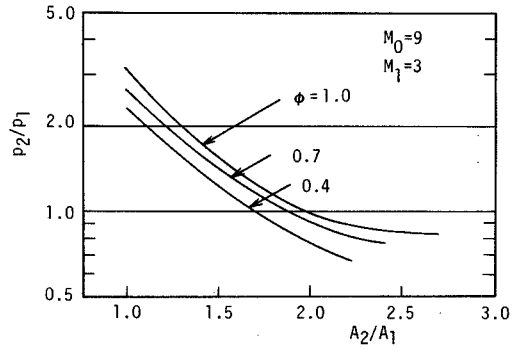

Fig. 12 Pressure ratio between combustor-inlet and exit.

equivalence ratio approaches unity, the optimum combustor-area-ratio increases. At β_C = 0, choking occurs at small combustor-inlet Mach number. The better engine performance is obtained for small equivalence ratio. Because large heat addition generates much total pressure loss. In supersonic combustion, the most severe problem is boundary layer separation due to inverse pressure gradient. Figure 12 shows the pressure ratio between combustor-inlet and exit. The increase of equivalence ratio raises the pressure ratio. The large combustor-area-ratio results better performance due to small pressure ratio.

3.3. Effects of flight Mach number

Figure 13 shows the maximum specific impulse vs. combustor-inlet Mach number. The specific impulse decreases monotonously with combustor-inlet Mach number. Because the greater losses of total pressure would result in the combustor than in the inlet. The performance are also degraded with the increase of the flight Mach number. The combustor-area-ratio optimized for combustor-inlet Mach number increases with the flight Mach number.

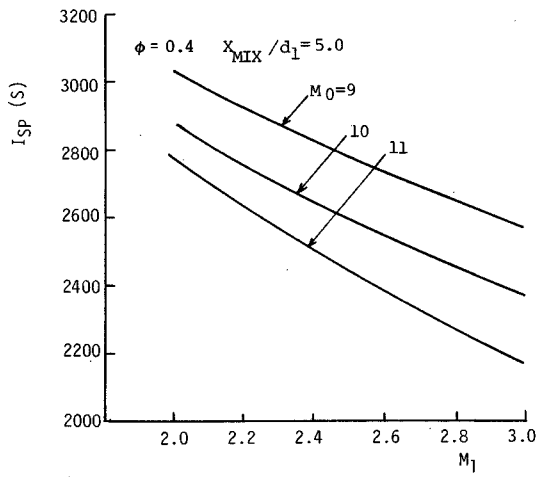

Fig. 13 Variation of maximum specific impulse with flight Mach number.

4. Concluding Remarks

The scramjet engines have been optimized using multiplier method. The quasi-one dimensional flow model is adopted for the combustor. The conclusions of this research can be summarized as follows.

1) The mixing of hydrogen and air is a rate-determining process. The axial length of the combustor is mainly determined by mixing rate.

2) The combustor-area-ratio can be optimized for combustor-inlet Mach number, which increases in keeping with the equivalence ratio.

3) Within the flight Mach number range, e.g. $M_0 = 9 - 11$, the total pressure loss in the combustor is larger than that in the inlet, so that the optimum performance corresponds to the case of the least loss in the combustor.

Nomenclature

A : cross-sectional area, m^2
d : diameter, m
E : energy of activation, kJ/kg
F : thrust, N
I_{sp} : specific impulse, s
h : enthalpy, kJ/kg or lower heating value, kJ/kg
K : equilibrium constant, –
k : reaction rate constant
$\dot{m}$: mass flow rate, kg/s
M_0 : flight Mach number, –
M : Mach number, –
r : radius, m
U : velocity, m/s
x : axial length of components, m
y : concentration of species, –
w : molecular weight of species, $g/mole$

Greek symbols

α : angle of divergence, deg
β : mach angle, deg or area-distribution rate, m^{-1}
γ : ratio of specific heats, –
θ : deflection angle, deg
λ : coefficient for modification of nozzle angle, –
ρ : density, kg/m^3
τ_w : shear stress, Pa
ϕ : equivalence ratio, –

Subscripts

a : air
C : combustor
f : fuel (hydrogen)

I : inlet
MIX : mixing
N : nozzle
p : combustion products
r : combustion reactants

References

1) P.J. Waltrup, F.S. Billig and R.D. Stockbridge, J. Spacecraft, **16**, 163 (1979).
2) F.S. Billig, 11th Sympo. on Combustion, 755 (1967).
3) Y. Tsujikawa, T. Sawada, M. Nagaoka and Y. Tsukamoto, Trans. JSME, **53**, 2219 (1987).
4) Y. Tsujikawa, T. Sawada, M. Nagaoka and Y. Tsukamoto, Trans. JSME, **53**, 2915 (1987).
5) R.C. Rogers and W. Chinitz, AIAA J., **21** 586 (1983).